Thermal and morphological studies of additively manufactured CFRP composites under thermal loadings

Isyna Izzal Muna *

Institute of Fluid-Flow Machinery, Polish Academy of Sciences
14 Fiszera Street, 80-231, Gdansk, Poland

Abstract

The aim of this experimental work is to study the thermal and morphological properties of carbon fiber reinforced polymer (CFRP) as polymeric composites printed using additive manufacturing via material extrusion. The printed samples were exposed to prolonged temperatures at 65°C, 145°C, 0°C and -20°C. Differential Scanning Calorimetry (DSC) was performed to analyze the thermal properties of CFRP composites and the scanning electron microscope (SEM) was utilized to study the morphological structure of the sample groups after thermal treatment. The specimens subjected to cyclic heating at hot temperatures have higher glass transition temperature (Tg) values than the prolonged groups. The visual examination of the morphological structure at the surface showed a slight deterioration in the morphological surface before and after thermal treatment at above-zero degrees Celcius. The higher the magnitude of the temperature treatment at above-zero degrees, the more damage is possessed in the polymer parts.

Keywords: CFRP composites; additive manufacturing; thermal characterization; morphological characterization; thermal treatment

1 Introduction

Carbon fiber reinforced polymeric (CFRP) composites are widely used in aerospace structures (tails, wings, fuselages), wind turbine blades, and marine engineering (boat construction) applications where structures must be lightweight, have exceptional mechanical strength, and withstand extreme environmental conditions. Rapid advancements in manufacturing techniques and the design of new materials and structures in the engineering sector have piqued the interest of industry and scientific research.

Additive manufacturing (AM) or three-dimensional (3D) printing, is a set of manufacturing techniques that allows for the layer-by-layer production of 3D components with complex geometries. Complex composite structures that are difficult to fabricate using traditional composite fabrication techniques can be easily manufactured with minimal expense, material waste, and machine setup time using 3D printing. With the necessity of building lightweight materials with high mechanical strength, AM can meet this demand. Fiber-reinforced thermoplastics have emerged as emerging materials in additive

*Corresponding Author. Email address: imuna@imp.gda.pl
https://doi.org/10.58139/wefn-t649

manufacturing due to their strength and stiffness without the need for multiple processes and special tools. For the matrix material, the advantage of employing thermoplastics such as polylactic acid (PLA), acrylonitrile butadiene styrene (ABS), polyether ether ketone (PEEK), etc in producing CFRP composites is their melt processability which can improve the manufacturing speed, lower the cost, and eliminate the prolonged cure cycles or complex curing chemistry. Another superiority of thermoplastics is that they can be manufactured using widely developed and readily available polymer AM methods.

During their life-time, understanding the effects of long-term thermal ageing is critical for better live performances of CFRP composites in order to avoid unexpected failure. A thorough understanding of the behavior of printing parts under constant thermal exposure can help predict their performance and serve to propose solutions for future improvements emerging in the industrial sectors. Many researchers have studied prolonged thermal effects on the mechanical properties of polymeric composites by applying thermal treatment at above zero degrees Celsius with most of the subjected parts manufactured using the traditional method [1–7]. Generally, the materials will undergo a lower strength at the macroscale due to induced micro-cracking of the matrix caused by thermal stress and chain-scission at the microscale. However, there is very little published data on the thermal treatment of 3D-printed polymer-based composites at subzero temperatures [8, 9]. So far, the researchers [10–14] have focused on sample parts printed with the FDM technique which were subjected to prolonged thermal exposure at above-zero temperatures. The aim of this paper is to characterize the morphological and thermal properties of 3D-printed composite parts after prolonged thermal treatment at various magnitudes. SEM micrographs reveal the porosity, defects, and damage within these structures which will indicate future directions for process optimization needed to obtain additively manufactured composite parts with desired properties.

2 Thermal analysis using DSC

2.1 DSC overview

The DSC method is a form of calorimetry, where the difference in heat flow between a test sample and a reference sample is measured during constant heating or cooling of the samples. Differential scanning calorimetry is a thermo-analytical technique that determines how much heat is required to raise a material's temperature. Differential scanning calorimetry (DSC) measures the energy absorbed (endotherm) or released (exotherm) as a function of time or temperature. It is used to characterize melting, crystallization, resin curing, loss of solvents, and other processes involving an energy change. Differential scanning calorimetry may also be applied to determine how much heat is required to raise a material's temperature processes (a change in heat capacity). Moreover, DSC rheology measurements are also suitable for detecting the effects of thermal degradation by observing the melting and crystallization process. Thermal degradation can also be observed through the complex viscosity which is very sensitive to chain modifications such as scission, branching, and cross-linking [15].

A DSC measuring cell consists of a furnace and an integrated sensor with designated positions for the sample and reference pans. The sample is placed in an aluminium pan, and the sample pan and an empty reference pan are placed on small platforms within the DSC chamber. Thermocouple sensors lie below the pans and they are connected to thermocouples. This allows for recording both the temperature difference between the sample and reference side (DSC signal) and the absolute temperature of the sample or

reference side. The functional principle of an interior chamber of DSC is shown in Fig.1.

DSC measurements can be made in two ways: by measuring the electrical energy provided to heaters below the pans necessary to maintain the two pans at the same temperature (power compensation), or by measuring the heat flow (differential temperature) as a function of sample temperature (heat flux). The DSC ultimately outputs the differential heat flow (heat/time) between your material and the empty reference pan. Heat capacity may be determined by taking the ratio of heat flow to the heating rate. Therefore, $C_p = \frac{q}{\Delta T}$ where C_p is the material's heat capacity, q is the heat flow through the material over a given time, and ΔT is the change in temperature over that same time.

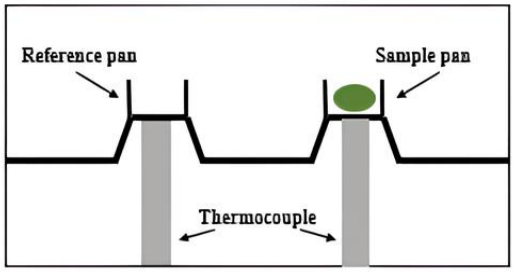

Figure 1: Schematic diagram of DSC interior chamber

Due to the heat capacity (C_p) of the sample, the reference side (usually an empty pan) generally heats faster than the sample side during the heating of the DSC measuring cell; for instance, the reference temperature (Tr, green) increases a bit faster than the sample temperature (Ts, green). The two curves exhibit parallel behavior during heating at a constant heating rate until a sample reaction occurs. In the case shown here, the sample starts to melt at t_1. The temperature of the sample does not change during melting; the temperature of the reference side, however, remains unaffected and continues exhibiting a linear increase. When melting is completed, the sample temperature also begins to increase again and, beginning with the point in time t_2, again exhibits a linear increase.

The differential signal (ΔT) of the two temperature curves is presented in the lower part of the image. In the middle section of the curve, the calculation of the differences generates a peak (blue) representing the endothermic melting process. Depending on whether the reference temperature was subtracted from the sample temperature or vice versa during this calculation, the generated peak may point upward or downward in the graphs. The peak area is correlated with the heat content of the transition (enthalpy in J/g). A typical DSC thermogram is shown in schematic Fig. 2 below.

2.2 DSC experimental procedure

Differential scanning calorimetry (DSC) was used to determine the glass transition temperature (Tg) of the polymeric composite samples in accordance with ASTM E1356. The melting temperature and crystallization temperature will also be analyzed according to ASTM E794. The purpose of the test was to determine whether there was any change in crosslinking of the PLA polymer, which could signify degradation as a result of the conditioning process. A DSC equipment (TA Instruments Q2000) was used to perform thermal analysis of the composite samples under controlled and isothermal conditions. The sample for each thermally treated group was chopped into small pieces to fit inside the pan due to the stiffness of the fiber-reinforced raw filament. There were 5 groups

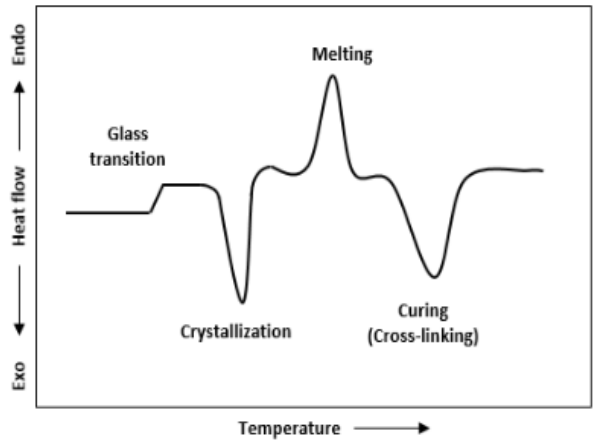

Figure 2: A schematic of a DSC thermogram

of printed CFRP samples for various thermal treatments as summarized in Tab. 1. The prepared samples then were measured with a precision scale. About 10 mg of sample from each treatment group was placed in an alumina hermetic pan and inserted into the DSC cell. A nitrogen atmosphere was supplied to the test chamber at a flow rate of 50 mL/min for the cooling process while an electrically heated furnace is used for heating. The temperature was ramped from 20°C to 200°C and then cooled back to 20°C at a heating and cooling rate of 10°C/min. The measurement for each sample consisted of two times of the heating process and one time of the cooling process. The following program was used: hold equilibrium at 24°C, ramp at 10°C/min to 200°C, hold isotherm for 2 min, ramp at 10°C/min to 40°C, hold isotherm for 2 min, and ramp back at 10°C/min to 200°C. The DSC equipment and DSC cell can be seen in Fig.3.

Table 1: Sample groups

Group name	Value
Intact	untreated samples
HS-A	hot stable at 65°C for 6 hours
HS-B	hot stable at 145°C for 6 hours
CS-A	cold stable at 0°C for 6 hours
CS-B	cold stable at -20°C, for 6 hours

Semicrystalline polymers are made up of two distinct phases: amorphous and crystalline. As a polymer becomes more crystalline, the fraction of the amorphous component decreases, and thus the change in the sample's C_p at Tg decreases. If the polymer becomes highly crystalline, the DSC instrument may eventually lose its sensitivity to detect Tg. In general, as the crystalline content of the polymer increases, so will the Tg temperature. The glass transition temperature is commonly abbreviated as Tg. Tg is the main characteristic transformation temperature of the amorphous phase and is produced by all

Figure 3: DSC equipment and DSC cell

amorphous (non-crystalline or semi-crystalline) materials during heating. When a hard, solid, amorphous material or component changes to a soft, rubbery, liquid phase, the glass transition phenomenon occurs. Tg is a valuable material characterization parameter that can provide very useful information about a product's end-use performance. The 'classic' Tg is observed as a stepwise endothermic change in the DSC heat flow or heat capacity.

2.3 DSC result analysis

Analysis of DSC curves for the initial heating, cooling, and second heating cycles of intact (untreated) and thermally treated CFRP specimens at stable and cyclic temperature modes are shown in Fig. 4. The important thermal phases such as glass transition (Tg), cold crystallization (Tcc), and melting point (Tm) temperature are studied to determine the polymer crystallinity. Glass transition temperature is indicated by a shift of the baseline from the initial DSC curves and reported glass transition temperature was based on the observed midpoint temperature. An exothermic peak indicates a cold crystallization where an exothermic reaction (heat release) has occurred, while an endothermic peak (heat adsorption) refers to the melting temperature in which an endothermic reaction takes place.

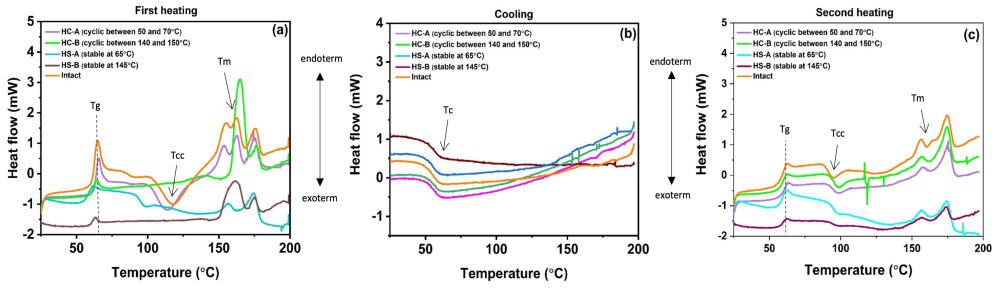

Figure 4: DSC graphs of 3D printed specimens: (a) First heating on thermally stable treatment groups; (b) Cooling on thermally stable treatment groups; (c) Second heating on thermally stable treatment groups

In the first heating process, the Tg of the untreated (intact) CFRP group falls at 65°C (midpoint) and is very much close to composites treated at a stable temperature at 0°C (CS-A). The specimens exposed to a stable subzero temperature at -20°C (CS-B) have slightly higher Tg compared to intact samples. The cold crystallization (Tcc) point of the intact group is observed to be the highest among treated groups indicated by an exothermal effect at a peak temperature of 117°C. Cold crystallization refers to the freezing of polymer chains in their amorphous state as a result of rapidly cooling a crystalline plastic from its liquid state. Crystallization is characterized by crystal nucleation and nucleus growth [16]. The cold crystallization process is distinguished by two characteristics: the promotion of nucleation as the supercooled glassy state gradually gains mobility with increasing temperature, and the presence of a maximum temperature for nucleation above which the cold crystallization process is diffusion limited [17]. The samples subjected to 65°C (HS-A group) have Tcc values of 98°C which is lower than the intact group. However, cold crystallization did not occur for the thermal group treated at 145°C (HS-B group) because the crystals do not have enough time to form. When reheating a material in this state, the formation of crystals causes an endothermic peak between the glass transition and the melting point.

In the first heating run, the double peak of melting temperatures was observed in all sample groups. This is due to the super-positioning of melting and recrystallization processes causing this behaviour. When the majority of the crystallization occurs during the cool-down process, the remaining amorphous regions lack place and chain mobility, resulting in imperfect crystals. These imperfect crystals begin to melt, but almost simultaneously, recrystallization occurs, resulting in the formation of a new crystal structure, which begins to melt almost immediately, forming the second peak [10]. During phase transitions, CFRP samples were observed to exhibit two distinct peaks (and onset points) which may indicate more than one form or crystal structure. Polylactic acid (PLA) is a polymer type used in the manufacturing process of CFRP composites and this thermoplastic has slow crystallization kinetics. In the case of PLA, three different crystallization processes can be identified with adequate experimental conditions: the classical cold crystallization and two processes associated with the non-reversing exotherms [18]. The DSC graphs obtained in this experiment exhibit unexpected and extraneous results such as non-reversing heat-flow curves with two exothermic processes and a larger endotherm in the middle. The multi-exothermic processes result from the occurrence of multiple crystalline states of PLA (α and β). The first peak at lower temperatures relates to the melting of the α crystalline state and its recrystallization into the α form, while the second peak at higher temperatures corresponds to the melting state β. The α - β phase transition is the transition from β to form following melting and recrystallization.

In the second heating process, the DSC curve produced lower values than the first run. The reason for this phenomenon is that the relaxation or molecular rearrangement already occurred in the first heating run, therefore the cooling process imparts/equilibrates the previously known history at a known rate from the first heating before heating again. As a result, any changes detected in the second heating curve between identical materials are due to actual internal differences in the materials (e.g., molecular weight) rather than previous thermal history effects. The cooling cycle gives the melt crystallization peak in each sample. The values of enthalpies obtained from the melting peak during the heating cycle and the melt crystallization peak during the cooling cycle are almost equal in each sample. This peak indicates the crystalline nature of the polymer. However, there are some cases when the reinforcement materials would constrain the PLA chains so much that the heat capacity jump becomes undetectable in DSC. Spatial confinement,

nucleation on sample boundaries, temperature gradient, and melt flow are all important factors in polymer crystallization. Similarly, the presence of foreign substances in the pure PLA matrix influences PLA crystallization by assisting or hindering chain mobility.

3 Morphological analysis using scanning electron microscope (SEM)

Scanning electron microscopy (SEM) observation was carried out to evaluate the microstructure of specimens due to thermal treatment and the degradation of the polymer matrix, fibers, and interface was qualitatively evaluated using this observation. SEM device FE-SEM SU5000, Hitachi Co., Tokyo, Japan was utilized to investigate the micro-structural damage that resulted from tensile testing on various specimen groups. The largest specimen that the SEM could detect had dimensions of 200 mm in diameter and 80 mm in height.

The SEM images after thermal treatment are shown in Fig. 5. According to the SEM micrographs, the effect of prolonged thermal treatment on the 3D-printed CFRP specimens caused different microstructural fracture damages after tensile testing in both the polymers and carbon fibers when compared to the untreated (intact) specimens. The polymer structure of the intact sample structure was morphologically unseparated, and there was no breakage. The PLA polymers treated with prolonged temperature at 65°C exhibit smaller cracks compared to the sample group treated at 145°C. In the cold thermal treatment case, the prolonged temperature at -20°C (CS-B) has created some noticeable gaps in the fibers, and matrix crack was also presented with some fiber pull-out. For the treatment at 0°C (CS-A) fibers seemed to remain in their initial arrangement and the gaps between fibers were not observed. However, the PLA matrix is slightly distorted compared to the untreated (intact) group.

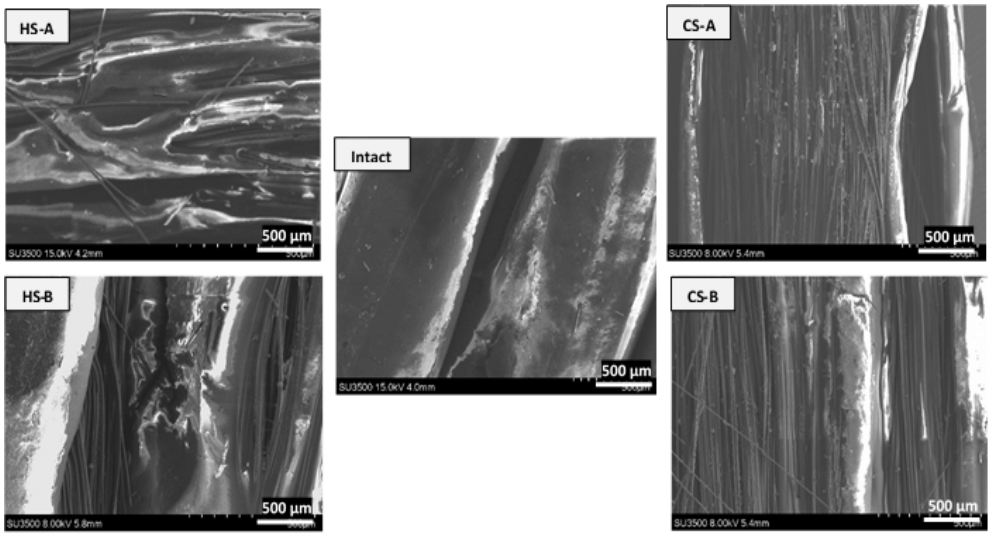

Figure 5: SEM photos of the untreated and treated specimen groups following destructive tensile testing.

4 Conclusion

In this paper, thermal and morphological characterization of additively manufactured CFRP composites under prolonged thermal loadings at above- and sub-zero temperatures were presented and discussed. After the manufacturing process, the thermal treatments at various magnitudes and modes were then subjected to the printed samples. Based on the thermal analysis using DSC testing, glass transition temperature (Tg), cold crystallization temperature (Tcc), and melting temperature (Tm) were studied. Cold crystallization did not occur when the specimens were exposed to the prolonged temperature at 145°C (HS-B group) because crystals are not given enough time to form. Since the cooling process equilibrates the previously known history at a known rate from the first heating before heating again, the first heating produced higher thermal values than the second heating run. As a result, any differences observed in the second heating curve between identical materials are due to actual internal material differences (e.g., molecular weight) rather than previous thermal history effects. During phase transitions, CFRP samples were found to have two distinct peaks (and onset points), indicating that they may have more than one form of crystal structure. The superpositioning of melting and recrystallization processes resulted in a double peak of melting temperatures. The visual inspection of the morphological surface shown in Fig. 5 revealed that the morphological surface changed slightly before and after the thermal treatment at subzero temperatures. The surface difference after the thermal treatment at above-zero temperatures is more noticeable.

The DSC curve confirmed a dried polymer matrix in the case of a CFRP sample exposed to continuous heating at 145°C by a smaller area of melting peak. The fracture interface of the 3D CFRP specimens, as well as changes in the matrix microstructure from each group, were examined using the SEM microscope. To investigate such outcomes, one specimen from each group that best reflected the failure mode was chosen. According to the findings, the higher the temperature exposure for above-zero degrees, the worse the damage in the polymer parts. The fibers had dried out during the heating process, making them more brittle than the groups that had been handled at lower temperatures. In the cold thermal treatment, a continuous temperature loading of -20°C (CS-B) caused some obvious gaps in the fibers, and a matrix break with some fiber pull-out was also seen. Fibers appeared to maintain their initial configuration during the 0°C (CS-A) treatment, and gaps between fibers were not seen.

5 Acknowledgement

The research was supported by the project entitled: Thermal degradation processes of additively manufactured structures (2019/35/O/ST8/00757) granted by the National Science Centre, Poland.

Received in June 2023.

References

[1] A. Ghasemi and M. Moradi, "Low thermal cycling effects on mechanical properties of laminated composite materials," *Mechanics of Materials*, vol. 96, pp. 126–137, 2016.

[2] M. Lafarie-Frenot and N. Ho, "Influence of free edge intralaminar stresses on damage process in cfrp laminates under thermal cycling conditions," *Composites Science and Technology*, vol. 66, no. 10, pp. 1354–1365, 2006.

[3] Z. Razak, A. B. Sulong, N. Muhamad, C. H. C. Haron, M. K. F. M. Radzi, N. F. Ismail, D. Tholibon, and I. Tharazi, "Effects of thermal cycling on physical and tensile properties of injection moulded kenaf/carbon nanotubes/polypropylene hybrid composites," *Composites Part B: Engineering*, vol. 168, pp. 159–165, 2019.

[4] C. Ma, D. Sánchez-Rodríguez, and T. Kamo, "Influence of thermal treatment on the properties of carbon fiber reinforced plastics under various conditions," *Polymer Degradation and Stability*, vol. 178, p. 109199, 2020.

[5] N. Hancox, "Thermal effects on polymer matrix composites: Part 1. thermal cycling," *Materials & Design*, vol. 19, no. 3, pp. 85–91, 1998.

[6] K. Shivakumar and A. Bhargava, "Failure mechanics of a composite laminate embedded with a fiber optic sensor," *Journal of composite materials*, vol. 39, no. 9, pp. 777–798, 2005.

[7] C. Lüders, D. Krause, and J. Kreikemeier, "Fatigue damage model for fibre-reinforced polymers at different temperatures considering stress ratio effects," *Journal of Composite Materials*, vol. 52, no. 29, pp. 4023–4050, 2018.

[8] O. Mysiukiewicz, M. Barczewski, and A. Kloziński, "The influence of sub-zero conditions on the mechanical properties of polylactide-based composites," *Materials*, vol. 13, no. 24, p. 5789, 2020.

[9] S. Kuciel, K. Mazur, and M. Hebda, "The influence of wood and basalt fibres on mechanical, thermal and hydrothermal properties of pla composites," *Journal of Polymers and the Environment*, vol. 28, pp. 1204–1215, 2020.

[10] M. Handwerker, J. Wellnitz, H. Marzbani, and U. Tetzlaff, "Annealing of chopped and continuous fibre reinforced polyamide 6 produced by fused filament fabrication," *Composites Part B: Engineering*, vol. 223, p. 109119, 2021.

[11] M. Zhang, B. Sun, and B. Gu, "Accelerated thermal ageing of epoxy resin and 3-D carbon fiber/epoxy braided composites," *Composites Part A: Applied Science and Manufacturing*, vol. 85, pp. 163–171, 2016.

[12] C. Pascual-González, P. San Martín, I. Lizarralde, A. Fernández, A. León, C. Lopes, and J. Fernández-Blázquez, "Post-processing effects on microstructure, interlaminar and thermal properties of 3D printed continuous carbon fibre composites," *Composites Part B: Engineering*, vol. 210, p. 108652, 2021.

[13] K. Wang, H. Long, Y. Chen, M. Baniassadi, Y. Rao, and Y. Peng, "Heat-treatment effects on dimensional stability and mechanical properties of 3D printed continuous carbon fiber-reinforced composites," *Composites Part A: Applied Science and Manufacturing*, vol. 147, p. 106460, 2021.

[14] Y. Ma, S. Jin, M. Ueda, T. Yokozeki, Y. Yang, F. Kobayashi, H. Kobayashi, T. Sugahara, and H. Hamada, "Higher performance carbon fiber reinforced thermoplastic composites from thermoplastic prepreg technique: Heat and moisture effect," *Composites Part B: Engineering*, vol. 154, pp. 90–98, 2018.

[15] M. Martín, F. Rodríguez-Lence, A. Güemes, A. Fernández-López, L. A. Pérez-Maqueda, and A. Perejón, "On the determination of thermal degradation effects and detection techniques for thermoplastic composites obtained by automatic lamination," *Composites Part A: Applied Science and Manufacturing*, vol. 111, pp. 23–32, 2018.

[16] E. Van Cappellen and A. Schmitz, "A simple spot-size versus pixel-size criterion for X-ray microanalysis of thin foils," *Ultramicroscopy*, vol. 41, no. 1-3, pp. 193–199, 1992.

[17] S. Vyazovkin, *Isoconversional kinetics of thermally stimulated processes*. Springer, 2015.

[18] C. A. Gracia-Fernández, S. Gómez-Barreiro, J. López-Beceiro, S. Naya, and R. Artiaga, "New approach to the double melting peak of poly (l-lactic acid) observed by DSC," *Journal of Materials Research*, vol. 27, no. 10, pp. 1379–1382, 2012.